CHAPTER II

STUDIES ON THE HYDROPHOBIC IONIC LIQUID WITH SUGAR-BASED NON-IONIC SURFACTANT MICROEMULSIONS: PHASE BEHAVIOUR AND MICROSTRUCTURE

Studies on the hydrophobic ionic liquid with sugar-based non-ionic surfactant microemulsions: phase behaviour and microstructure

Microemulsions have been investigated as a novel and adaptable reaction medium for a wide range of chemical reactions. including preparation of nanoparticle, organic synthesis, bio-organic synthesis, and so on. The phase behaviour and microstructure of a ternary microemulsion system comprising sugar-based non-ionic surfactant/1-butyl-3-methylimidazolium hexafluorophosphate/water, were investigated as a function of temperature and sugar surfactant mass fraction, γ. for a ternary microemulsion system involving sugar-based non-ionic surfactant/1-butyl-3-methylimidazolium hexafluorophosphate/water. In the present work, a hydrophobic room temperature ionic liquid (RTIL), 1-butyl-3-methylimidazolium hexafluorophosphate was utilized instead of organic solvents (*n*-alkanes) as an oil/non-polar phase in a ternary microemulsion formulations, wherein a sugar-based alkyl polyglycoside non-ionic surfactant was used as a substitute for the conventional non-ionic surfactant (i.e. alkyl polyoxyethylene ether class) in order to solubilize the hydrophobic ionic liquid and water. The capability of non-ionic sugar-based surfactant *n*-decyl β-D-maltoside, and *n*-dodecyl β-D-maltoside, to solubilize oil (hydrophobic ionic liquid) and water, i.e., $\overline{X}$ was evaluated. Furthermore, the change in specific conductivity of microemulsions as a function of volume fraction was explored in depth to extract information about the percolative or anti-percolative behaviour of microemulsions. Lastly, we have also studied the phase behaviour for a ternary microemulsion system involving industrial-grade sugar-based lauryl glucoside (and) cocamidopropyl betaine zwitterionic surfactant/ 1-butyl-3-methylimidazolium hexafluorophosphate/water.

2.1   Introduction

Microemulsions are optically clear dispersions made up of at least three ingredients: two immiscible liquids and a surfactant. Amongst this, water, oil, and surfactant mixtures exhibit a wide range of microstructures inside the single-phase microemulsion domains, as well as a of liquid crystalline or mesomorphic phases, in addition to other types of multiple-phase systems (Qiu & Texter, 2008;Winsor, 1948; Kuchlyan et al., 2016; Anjum et al., 2009; Sjöblom et al., 1996; Hejazifar et al., 2020; Bellocq et al., 1984; Kahlweit, 1999; Atkin & Warr, 2007). Based on the type of surfactant utilised and the type of sample environment, microemulsions are classified as water-in-oil (w/o), oil-in-water (o/w), or bicontinuous systems (Winsor, 1948;

Rakshit et al., 2019). Low interfacial tension between the oil and water phases distinguishes them. When the surfactant is present in a monomeric state at low concentrations, the surfactant-rich oil phases coexist with the surfactant-poor aqueous phase in w/o microemulsions, whereas the surfactant-rich water phase coexists with the oil phase in o/w microemulsions (Kuchlyan et al., 2016). The surfactants, as well as co-surfactants in some cases, help to keep nanostructured water-oil mixtures stable. The surfactant forms a monolayer between the two immiscible liquids (water and oil), which reduces the interfacial tension. The bicontinuous microemulsions develop when the interfacial tension is zero, and surfactant monolayers separate into disordered, interpenetrating oil and water domains (Anjum et al., 2009).

Because their structure can be easily adjusted systematically and film curvature can be tuned by simply increasing the temperature, non-ionic alkyl polyoxyethylene ether surfactants, also known as C_iE_j surfactants, are commonly used to study the physical properties of microemulsions. As a consequence, it allows for a simple and methodical analysis of the specific structures that are been generated (Kahlweit et al., 1990; Stubenrauch, 2009). Researchers are in the quest for alternatives to organic solvents because of the dangers they pose to the environment (Lyklema, 2005; Rogers, 2003; Zech et al., 2010). RTILs are solvents that are only made up of ions and are liquid at room temperature. RTILs have organic and inorganic positive ions (cations) and negative ions (anions) (Rogers, 2003; Zech et al., 2010a; Marsh et al., 2004; Pramanik et al., 2011). By altering the cationic and anionic constituents, which can be tuned according to the needed qualities that enable the dissolution of numerous sparingly soluble substrates, it is possible to synthesise RTILs possessing appropriate properties.

As a result, ionic liquids have been dubbed as 'designer solvents' (Pramanik et al., 2011), and they are frequently utilized as a green alternative to traditional volatile organic solvents owing to their unique properties such as near-zero vapour pressure, non-volatility at high temperatures, a wide electrochemical window, non-flammability, and high thermal stability (300°C or more), and wide liquid range (Plechkova, 2007; Marsh et al., 2002). As a result, ionic liquids have been competently utilized to substitute either water or organic solvents in a microemulsion. In a microemulsion, the polar phase is usually water, while the non-polar phase is usually an organic solvent (*n*-alkanes are commonly utilised) (Hallett & Welton, 2011; Thater et al., 2014; Thater et al., 2019; Rai & Pandey, 2014; Mandal et al., 2013; Porada et al., 2017). The length of the alkyl groups introduced into the cation can also be modified, resulting in a systematic and controlled modification in their properties. As a result, RTILs can be

employed as either the hydrophilic or hydrophobic phase, implying that they can be used as solvents in microemulsion systems (Porada et al., 2017; Han, 2005; Atkin & Warr, 2007; Gao et al., 2004; Ghosh et al., 2013).

Ionic liquids have also been used for the formulation of a microemulsion as one of the three components: water-like solvents, hydrophobic solvents, and as surfactants (Porada et al., 2016; Gao et al., 2007; Gao et al., 2005; Li et al., 2006; Kumar & Mittal, 1999; Kunz et al., 2012). It has been found that substantially larger surfactant concentrations are required to stabilise an ionic liquid microemulsion compared to equivalent aqueous systems (Porada et al., 2016; Gao et al., 2007; Li et al., 2006; Porada et al., 2011). According to a review of few literature experiments, the structural changes within the microemulsion phase as a function of surfactant concentration and temperature were unknown, and the ternary phase behaviour of ionic liquid microemulsions was poorly characterised (Gao et al., 2007; Li et al., 2006; Gao et al., 2006; Gao et al., 2005).

RTILs have been used as reaction media in a number of studies (Gao et al., 2007; Li et al., 2006; Gao et al., 2005), but their application is limited owing to their ability to dissolve a large number of solute molecules. Hence, a non-polar solvent can be used as a co-solvent or ionic liquid-in-oil microemulsions containing hydrocarbon domains to tackle this problem. It has been mentioned in several research articles about the microemulsion systems where an ionic liquid is employed instead of a water as a polar phase or as replacement of oil phase (Porada et al., 2016; Gao et al., 2007; Hao & Zemb, 2007). There has been a significant increase in the number of studies on microemulsions using ionic liquid as one of the components from both theoretical (thermodynamics, particle interactions) and practical (possible use as novel reaction media) perspectives (Hao & Zemb, 2007; Gao et al., 2009; Atkin & Warr, 2005; Bilgili et al., 2016; Najjar et al., 2020). The self-assembly of surfactants in microemulsions using ionic liquids rather than water or organic solvents has been extensively studied (Qiu & Texter, 2008; Kuchlyan et al., 2016; Hao & Zemb, 2007; Atkin & Warr, 2005). On the other hand, the inclusion of octanol as a co-surfactant did not increase the efficiency of the ionic liquid microemulsion system, and the efficiency is too low for technological applications (Porada et al., 2011).

The proposed research is further driven by the fact that when using typical non-ionic alkyl polyglycol ether (C_iE_j) surfactants to make a microemulsion, the surfactant concentration required to solubilize similar quantities of water and a hydrophobic ionic liquid is 30-45 percent

(Anjum et al., 2009; Atkin & Warr, 2007; Porada et al., 2017; Porada et al., 2011). Furthermore, non-ionic surfactants of the alkyl polyglycol ether (C_iE_j) family have a strong temperature influence on microemulsions, making them unsuitable for formulating systems that are stable over a large temperature range (Zech et al., 2009; Zech & Bauduin et al., 2010; Zech et al., 2010). The ability to increase the traditional thermal stability range of microemulsions at ambient pressure is a major property of ionic liquids in microemulsions. As a result, non-aqueous microemulsions containing ionic liquids can be created with a thermal stability range of 30°C to 150°C (Zech, et al., 2010). Temperature has little effect on the physicochemical properties of sugar surfactant aqueous solutions.

In the formulation of ternary microemulsion systems containing water/ IL/ surfactant, hydrophobic ionic liquids such as 1-butyl-3-methylimidazolium hexafluorophosphate [Bmim][PF_6] have also been utilised to substitute organic solvents (Li et al., 2005; Gao et al., 2005; Zheng & Eli, 2009; Anjum et al., 2009; Porada et al., 2017; Kusano et al., 2014; Porada et al., 2016; Porada et al., 2011). Gao et al. (2005) prepared and characterized water/[Bmim][PF_6]/TX-100 ternary system but the phase diagram and microstructure were not studied. Three types of microstructures were found in the ternary water/[Bmim][PF_6]/ Tween-20 9 (Gao et al., 2006; Zheng & Eli, 2009) microemulsion system. Seth et al. (2007) examined the interaction of the ionic liquid with water using the same water/ [Bmim][PF_6]/ TX-100 microemulsion system.

All of the studies listed above were conducted at room temperature. Following that, the phase diagram and microstructure of ternary water/ [Bmim][PF_6]/ TX-100 microemulsion as a function of temperature and surfactant mass fractions were then investigated. However, there hasn't been yet a comprehensive study showing the preparation and phase behaviour of microemulsion systems comprising ionic liquid/s, water, and industrial-grade sugar-based lauryl glucoside (and) cocamidopropyl betaine surfactant in past studies. As a result, here, the current study focused on the phase behaviour and microstructure of a ternary system of water/1-butyl-3-methylimidazolium hexafluorophosphate/sugar surfactant as a function of temperature and sugar surfactant mass fraction, γ. To begin, a hydrophobic ionic liquid 1-butyl-3-methylimidazolium hexafluorophosphate was utilised as an oil/non-polar phase substitution in ternary microemulsion formulations to replace commonly used organic solvents (*n*-alkanes). To solubilize hydrophobic ionic liquid and water, a sugar-based alkyl polyglycoside non-ionic surfactant was used instead of a standard non-ionic surfactant (i.e., alkyl polyoxyethylene ether class).

Secondly, in place of conventional surfactant, we developed a microemulsion system using industrial-grade sugar-based lauryl glucoside (and) cocamidopropyl betaine zwitterionic surfactant. The developed microemulsion systems were compared to those reported in the literature. In addition to this, we have also formulated microemulsion systems by substituting alkyl polyglycol ether (C_iE_j) surfactants in a ternary system with "green alternatives," such as alkyl glycoside or sugar surfactants (C_nG_m) that are stable across a wide temperature range. The new research also intends to lower the amount of sugar-based surfactant needed to dissolve the two immiscible liquids (Ionic Liquid and water).

Furthermore, numerous changes in the characteristics of the microemulsion have been documented in the literature(Dogra & Rakshit, 2004; Lagues & Sauterey, 1980; Borkovec et al., 1988; Jeirani et al., 2013; Li et al., 2007; Ponton et al., 1991b; Chen & Zhao, 2014; Jeirani et al., 2012; Garti, 2003; Schrodle et al., 2005) as the water content is increased. The static percolation approach and the dynamic percolation method were devised to characterise the electrical conductivity of various systems. However, in each case, the electrical conductivity was investigated as the physical features of the droplets, such as their size, fluctuated in tandem with the droplet concentration. As a result, the electrical conductivity measurements for the above-formulated microemulsions systems were discussed in this chapter. When the concentration of droplets rises, the electrical conductivity increases by five orders of magnitude. A percolation transition has been used to characterise this variation: beyond a critical volume concentration of droplets, an infinite path via aggregated droplets exists.

2.2   *Materials and methods*

The sugar surfactant *n*-dodecyl *β*-D-maltoside ($C_{24}H_{46}O_{11}$, purity $\geq 98\%$); *n*-decyl *β*-D-maltoside ($C_{22}H_{42}O_{11}$, purity $\geq 98\%$); non-ionic surfactant Triton X-100 ($C_{14}H_{22}O(C_2H_4O)n$, purity$\geq 97.0\%$); the Ionic liquid 1-butyl-3-methylimidazolium hexafluorophosphate [Bmim][PF$_6$] ($C_8H_{15}F_6N_2P$, purity $\geq 97.0\%$) was procured from Sigma Aldrich, USA (Solanki & Patil, 2021). The industrial-grade alkyl glucoside surfactant, PLANTACARE$^\circledR$ 810 – UP, i.e., C_{8-10} fatty alkyl glucoside or UP-810 and Lauryl Glucoside (and) Cocamidopropyl Betaine (PLANTACARE$^\circledR$ K-55) was received as a gift sample from BASF, Germany (Solanki & Patil, 2020).

Phase Studies

In order to examine microemulsions, it is necessary to study the phase behaviour of the formulated ternary system. By passing "slices" through the phase prism at a 1:1 water to hydrophobic ionic liquid (oil) ratio, or polar ionic liquid to solvent (oil) ratio, i.e., polar/ apolar 1:1, while varying the surfactant concentration, the phase behaviour of self-assembling ternary mixtures (water, hydrophobic ionic liquid, and non-ionic surfactant) has been studied as a function of temperature and composition (Atkin & Warr, 2007; Anjum et al., 2009; Solanki & Patil, 2020; Solanki & patil, 2021).

In test tubes, microemulsions were made by weighing known quantities of water, hydrophobic ionic liquid, and surfactant, or polar ionic liquid, solvent (oil), and surfactant. The sealed test tubes were immersed in a transparent heating circulator equipped with a water bath ($\pm$ 0.2 ℃). Visual inspection and optical polarised microscopy were used for identifying phase boundaries at temperatures ranging from 30 to 60°C, i.e., 1∅ (corresponding to one phase), 2∅ (corresponding to lower two-phase) or water/ionic liquid droplet microemulsion, 2∅ (corresponding to upper two-phase) or ionic liquid/water droplet microemulsion), and 3∅ (corresponding to three-phase regions) (Solanki & Patil, 2020; Solanki & patil, 2021).

The mass fraction of ionic liquid (α) in the solvent combination is used to define the ternary mixture sample compositions and is calculated by,

$$\alpha = \frac{m_{[\text{Bmim}][\text{PF}_6]}}{m_{[\text{Bmim}][\text{PF}_6]} + m_{\text{H2O}}}$$

as well as in the whole mixture as a surfactant mass fraction (γ) is calculated by,

$$\gamma = \frac{m_{\text{surfactant}}}{m_{[\text{Bmim}][\text{PF}_6]} + m_{\text{H2O}} + m_{\text{surfactant}}}$$

The phase boundaries give rise to a distinct "fish" outline illustrated in Figure 1.
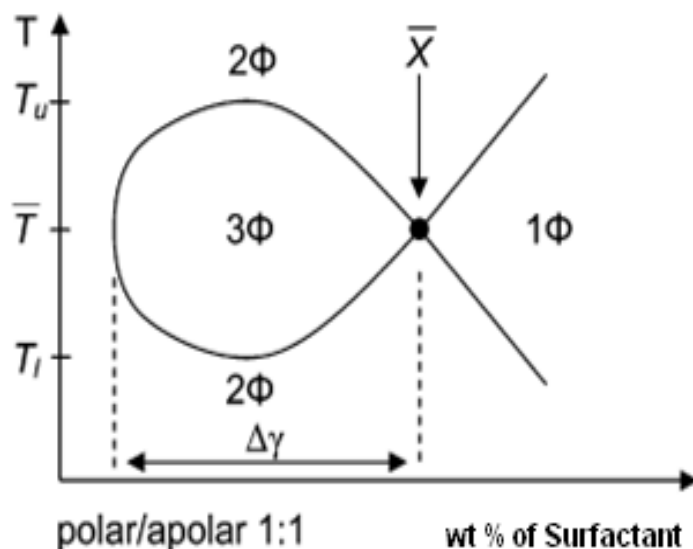

Figure 1. One phase 1∅), two phases (2∅), and three-phase (3∅) regions are shown in a schematic fish-shaped phase diagram obtained by cutting a vertical section through the phase prism for equal amounts of polar and apolar solvent. T represents the temperature of the system whereas the mass fraction of surfactant in the whole mixture is denoted by 'γ' (Tessendorf, 2007).

Figure 1 reveals that at T= $\bar{T}$ temperature and a very low surfactant concentration ($\gamma < \gamma_0$), the oil (ionic liquid) and water phases are at intermediate temperatures. As a result, the surfactant will be more soluble in both the water and oil (ionic liquid) phases, resulting in a surfactant-rich middle phase with an excess of oil and water in balance (Tessendorf, 2007). As the temperature rises, the intermediate phase expands as well, until it can hold all of the water and oil, giving rise to $\bar{X}$ or $\bar{\gamma}$ point, which is the surfactant concentration needed to dissolve equal amounts of ionic liquid in the oil phase and water in the non-polar phase.

At low temperatures, the lower phase (2∅) is the water-rich phase and the upper phase (2∅) is oil (ionic liquid)-excess phase, where the surfactant will form oil-swollen micelles also called microemulsion droplets. When a surfactant is added to this binary mixture, it becomes solubilized in both phases. Later, as more amount of surfactant is added, the concentration of the surfactant rises to surfactant mass fraction, i.e., $\gamma = \gamma_0$, and it is observed that both the oil and water phases are saturated at the fish head. With the addition of more surfactant, the third phase, the middle phase (3∅), appears (Tessendorf, 2007).

As the temperature rises, the surfactant becomes more soluble, until the three-phase region ($3\emptyset$) ($\gamma < \bar{\gamma}$) is reached. The addition of more surfactant reduces the interfacial tension between the phases, resulting in the formation of a one-phase region ($1\emptyset$) ($\gamma > \bar{\gamma}$) as shown in Figure 1. Ionic liquid (oil) is a superior solvent at higher temperatures, and IL-swollen reverse micelles form in an oil continuous phase, in equilibrium with an excess IL lower phase. The phase diagram interpreted in Figure 1 (Atkin & Warr, 2007) was used to determine the characteristic parameters ($\bar{T}$, $\bar{X}$,) of the microemulsion system.

Polarization Microscopy

The prepared microemulsion samples were placed on a glass slide, a coverslip was placed over the glass slide, and the sample was examined using a Leica DM750 P Polarization microscope with crossed polarizers.

Percolation Studies

Electrical conductivity measurements of a typical w/o or o/w microemulsion system were performed to gain insights regarding the system's percolative behaviour, i.e., dynamic percolation (structural transitions from water in ionic liquid dispersion through bicontinuous microstructure towards the water in ionic liquid microemulsion). Hanna (HI5321-02) research grade benchtop EC/TDS/resistivity/salinity metre capable of millesimal measuring resolution of conductivity with an extended range of 0.001 S/cm to 1 S/cm was employed for the electrical conductivity measurements.

In this study, we weighed an equal amount of PLANTACARE® 810 – UP, a sugar-based non-ionic surfactant, and 1-butyl-3-methylimidazolium hexafluorophosphate [Bmim][PF_6], a room temperature ionic liquid. The conductivity water was added by varying the volume mass fraction, and the corresponding conductance for each system was measured. Finally, the graph is plotted for conductance versus % of water. The differential plot (d ln σ/d ϕ_w), which shows a peak corresponding to ϕ_w (volume fraction of water), is usually used to determine the threshold volume fraction ($\emptyset_w^p$) of the dispersed phase required for the onset of percolation (volume fraction of water). Hait et al. (2001) proposed the use of the sigmoidal Boltzmann equation (SBE) for determining the threshold volume ($\emptyset_w^p$) two decades ago, in 2001.

The following is the equation.

$$\log \sigma = \frac{\log \sigma_i - \log \sigma_f}{1 + \exp\left(\phi_w - \phi_w^p\right)/d\phi_w} + \log \sigma_f$$

Here σ and ϕ_w represent the conductance and volume fraction of water whereas the subscripts i, f, and p are for initial, final, and percolation stages, respectively.

2.3   Results and discussion

Phase behaviour and Microstructure studies

Owing to its many favourable qualities, in a ternary water/oil/sugar-based non-ionic surfactant microemulsion system, a hydrophobic ionic liquid (e.g., 1-butyl-3-methylimidazolium hexafluorophosphate [Bmim][PF$_6$]) was employed to replace conventional organic solvents (*n*-alkanes). The microemulsion system with Triton X-100 (TX-100), water, and a hydrophobic ionic liquid (e.g., 1-butyl-3-methylimidazolium hexafluorophosphate [Bmim][PF$_6$]) was compared to the microemulsion system with PLANTACARE®810–UP(UP-810), a non-ionic sugar-based surfactant. The $\bar{X}$ value, i.e., the surfactant required to solubilize oil and water, is high (0.57), when employing a standard non-ionic surfactant like Triton X-100, as illustrated in Figure 2. Similarly, replacing the traditional non-ionic surfactant with PLANTACARE®810–UP, a sugar-based nonionic surfactant, reduces the $\bar{X}$ value to 0.46, as illustrated in Figure 3.

Table 1 lists the distinctive parameters of the fish-shaped phase diagrams of the following systems: 1) Triton X-100/[Bmim][PF$_6$]/water and 2) PLANTACARE®810–UP (UP-810)/[Bmim][PF$_6$]/water. The co-ordinates of the so-called fish head (lowest surfactant concentration at which a third middle phase appears) are γ_0 and T_0, whereas those of the fishtail (lowest surfactant concentration at which one phase is formed) is $\bar{\gamma}$ and $\bar{T}$, respectively for Triton X-100/[Bmim][PF$_6$]/water with that of PLANTACARE®810–UP (UP-810)/[Bmim][PF$_6$]/water, it is clear that the former microemulsion system formulated with conventional non-ionic surfactant has lower surfactant efficiency than the microemulsion formulated with sugar-based non-ionic surfactants.

It is evident from the experimental data that when employing the sugar surfactant to formulate the microemulsion system, there is a reduction in the amount of surfactant used when compared to the traditional surfactant.
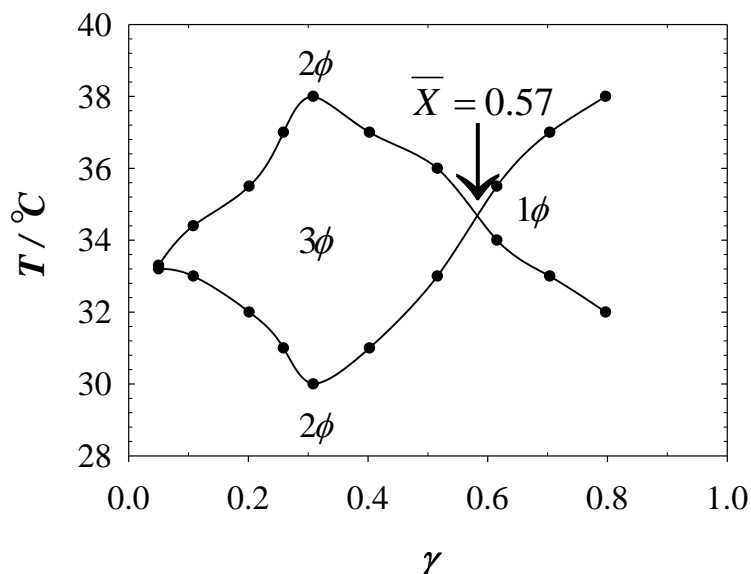
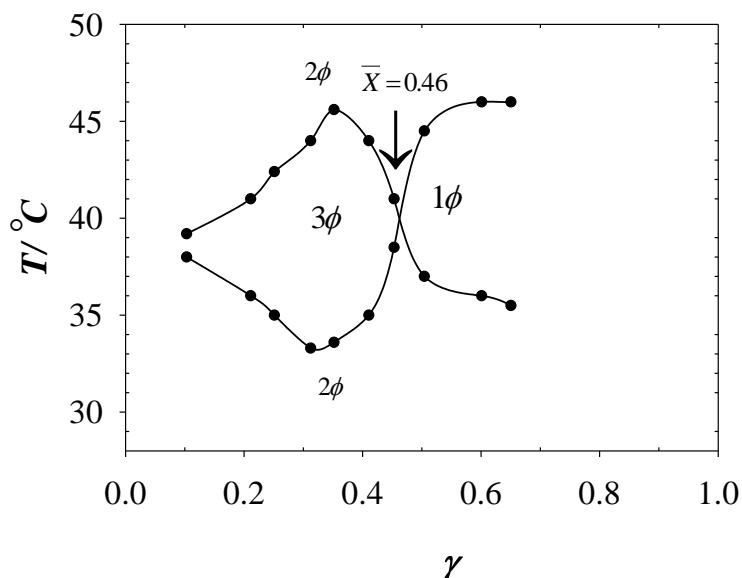**Figure 2**. Fish-shaped phase diagram obtained for equal masses of water and IL [Bmim][PF$_6$], in presence of non-ionic surfactant, i.e., Triton X-100/[Bmim][PF$_6$]/ H$_2$O. The chosen IL mass fraction α corresponds to equal volumes of water and IL. T/°C represents the temperature and γ is the mass fractions of surfactant. 1Ø corresponds to one phase, 2Ø corresponds to lower two-phase (W/IL droplet μE), 2Ø corresponds to upper two-phase (IL/W droplet μE), and 3Ø corresponds to three-phase regions, respectively.

Figure 3. A fish-shaped phase diagram depicted for equal masses of water and IL [Bmim][PF$_6$], in presence of non-ionic sugar-based surfactant, i.e., PLANTACARE®810–UP (UP-810)/ [Bmim][PF$_6$]/H$_2$O. The chosen IL mass fraction α corresponds to equal volumes of water and IL. T/°C represents the temperature and γ is the mass fractions of surfactant. 1Ø

corresponds to one phase, 2∅ corresponds lower two-phase (W/IL droplet μE), 2∅ corresponds upper two phases (IL/W droplet μE), and 3∅ corresponds to three-phase regions, respectively.

Table 1. Characteristic parameters of the constructed Phase diagrams

Microemulsion System	∅	γ_0	T_0/°C	$\overline{\gamma}$	$\overline{T}$/°C	$\Delta\gamma$	ΔT/°C
Triton X-100 / [Bmim][PF$_6$]/ H$_2$O	0.5	0.05	33.2	0.57	34.7	0.52	8.1
PLANTACARE®810–UP/ [Bmim][PF$_6$]/ H$_2$O	0.5	0.09	38.6	0.46	39.9	0.37	14.0

IL volume fraction ∅; coordinates of fish head γ_0, T_0; coordinates of fishtail $\overline{\gamma}$, $\overline{T}$; maximum extension of surfactant concentration and temperature of the 3-phase body $\Delta\gamma$, ΔT.

The capability of non-ionic sugar-based surfactant *n*-decyl β-D-maltoside (β-C$_{10}$G$_2$), and *n*-dodecyl β-D-maltoside (β-C$_{12}$G$_2$) required for solubilization of hydrophobic ionic liquid and water, i.e., $\overline{X}$ was evaluated. It is well known that the efficiency of a microemulsion increases with increasing surfactant alkyl chain length in water/*n*-alkane/C_iE_j systems (Dubois & Zemb, 2000; Kahlweit et al., 1988; Kahlweit et al., 1989; Kahlweit & Strey, 1987; Kahlweit, 1999). The microemulsion system comprising of sugar-based non-ionic surfactant/1-butyl-3-methylimidazolium hexafluorophosphate [Bmim][PF$_6$]/water exhibited a consistent pattern.

As shown in Figure 4, the $\overline{X}$ or $\overline{\gamma}$, was found to be 0.42 for the ternary microemulsion system, *n*-Decyl-β-D-maltoside (β-C$_{10}$G$_2$)/1-butyl-3-methylimidazolium hexafluorophosphate [Bmim][PF$_6$]/H$_2$O whereas Figure 5 shows that the $\overline{X}$ or $\overline{\gamma}$ was found to be 0.35 for *n*-Dodecyl-β-D-maltoside (β-C$_{12}$G$_2$)/1-butyl-3-methylimidazolium hexafluorophosphate [Bmim][PF$_6$]/H$_2$O microemulsion system. Table 2 shows the results corresponding to the formulated microemulsions' distinctive parameters. Figures 4 and 5 show that increasing the alkyl chain length of the surfactant from 10 to 12, i.e., β-C$_{10}$G$_2$ to β-C$_{12}$G$_2$, results in a 7% improvement in surfactant efficiency. Although it is expected that $\overline{T}$ decreases as the length of the surfactant alkyl chain increases, no apparent pattern could be ascertained in the variation of $\overline{T}$ in microemulsion system made with sugar-based non-ionic surfactants.
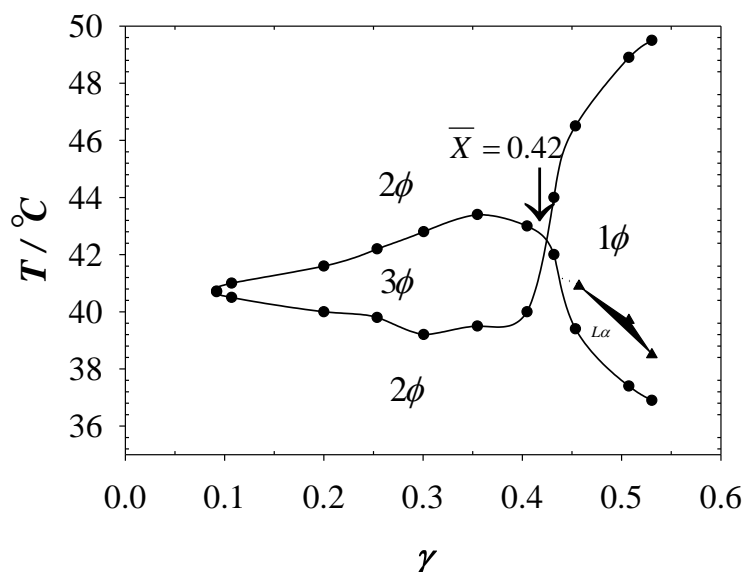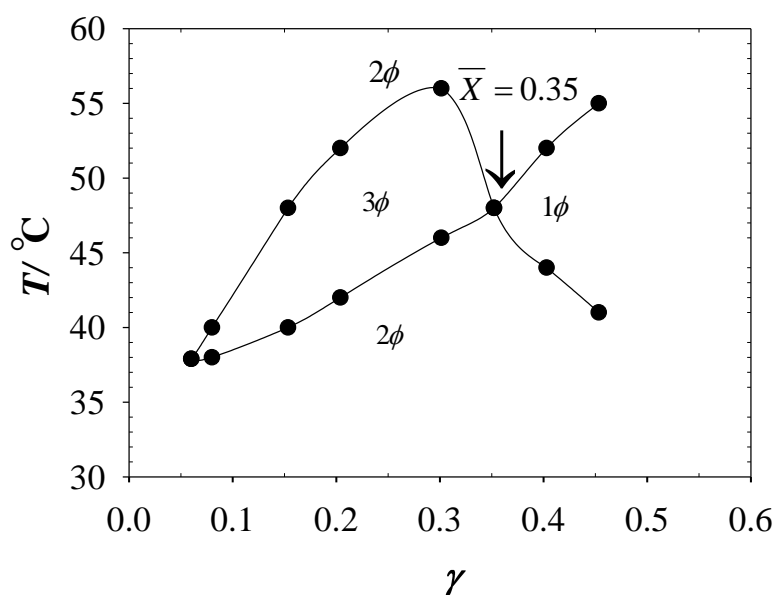
.

Figure 4. Fish-shaped phase diagram obtained for equal masses of water and IL [Bmim][PF$_6$], in presence of different non-ionic sugar-based surfactant, i.e., *n*-Decyl *β*-D-maltoside(*β*-C$_{10}$G$_2$)/ [Bmim][PF$_6$] / H$_2$O. The chosen IL mass fraction α corresponds to equal volumes of water and IL. T/°C represents the temperature and γ is the mass fraction of surfactant.

Figure 5. Fish-shaped phase diagram obtained for equal masses of water and IL [Bmim][PF$_6$], in presence of different non-ionic sugar-based surfactant, i.e., Dodecyl *β*-D-maltoside (*β*-C$_{12}$G$_2$)/[Bmim][PF$_6$]/ H$_2$O. The chosen IL mass fraction α corresponds to equal volumes of water and IL. T/°C represents the temperature and γ is the mass fraction of surfactant. 1∅ corresponds to one phase, 2∅ corresponds to lower two-phase (W/IL droplet μE), 2∅

corresponds to upper two-phase (IL/W droplet μE), and 3$\emptyset$ corresponds to three-phase regions, respectively.

It is evident from Figures 5 and 6, that the longer chain length of *n*-decyl β-D-maltoside (β-C$_{12}$G$_2$) moves the position of the fish head to a lower γ value when compared to *n*-decyl β-D-maltoside (β-C$_{10}$G$_2$). This result is in close agreement to those reported in the literature for TX-100/[Bmim][PF$_6$]/H$_2$O and C$_{14}$E$_4$/[Bmim][PF$_6$]/ H$_2$O microemulsion systems. It's worth noting that the lengthening of the alkyl chain has no influence on $\Delta\gamma$, which basically stays the same, whereas, ΔT increases dramatically. This behaviour contradicts the findings for the water/[Bmim][PF$_6$]/TX-100 ternary system (Gao et al., 2009). Polarization microscopy experiments were also carried out to gain a better understanding of the microstructure of sugar surfactant/ [Bmim][PF$_6$]/water microemulsions.

Figures 6 and 7 represent the polarisation microscopy images of for β-C$_{10}$G$_2$/[Bmim][PF$_6$]/H$_2$O and β-C$_{12}$G$_2$/[Bmim][PF$_6$]/ H$_2$O. At lower temperatures, both microemulsion systems showed lamellar liquid crystalline phases (L$_\alpha$) phases. The (L$_\alpha$) phases, on the other hand, do not entirely stretch and inhibit the 1-phase microemulsion, allowing precise phase boundary determination.

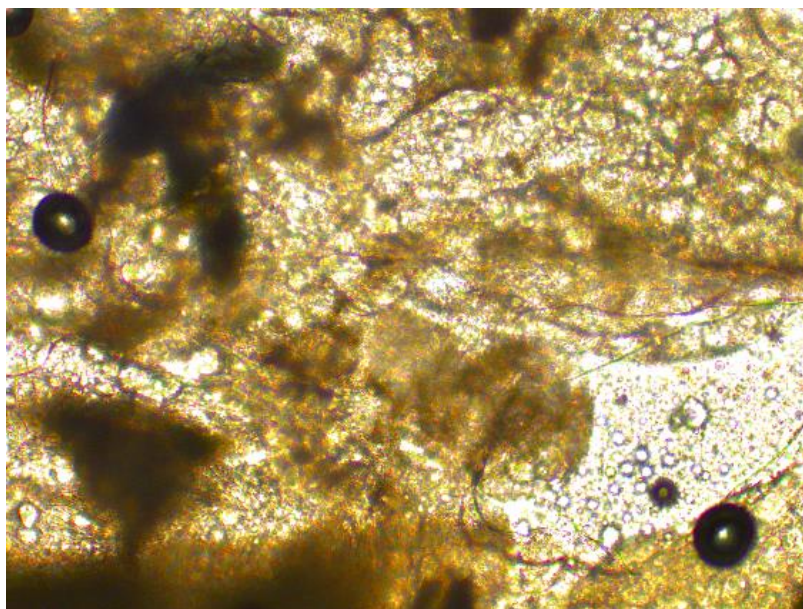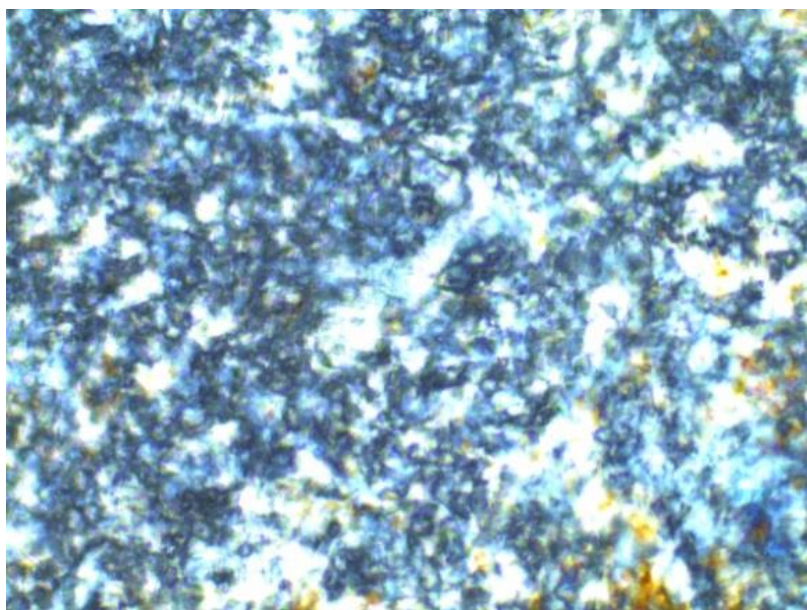**Figure 6**.   Polarization microscopy studies revealing the presence of L$_\alpha$ for β-C$_{10}$G$_2$/[Bmim][PF$_6$]/H$_2$O

Figure 7. Polarization microscopy studies revealing the presence of L_α for β-$C_{12}G_2$/[Bmim][PF$_6$]/H$_2$O

Table 2: Characteristic parameters of the constructed Phase diagrams

Microemulsion System	$\emptyset$	γ_0	T_0/°C	$\overline{\gamma}$	$\overline{T}$/°C	$\Delta\gamma$	ΔT/°C
β-$C_{10}G_2$ / [Bmim][PF$_6$]/ H$_2$O	0.5	0.09	40.7	0.42	42.6	0.33	3.9
β-$C_{12}G_2$ / [Bmim][PF$_6$]/ H$_2$O	0.5	0.05	37.8	0.35	47.7	0.30	2.0

IL volume fraction $\emptyset$; coordinates of fish head γ_0, T_0; coordinates of fishtail $\overline{\gamma}$, $\overline{T}$; maximum extension of surfactant concentration and temperature of the 3-phase body $\Delta\gamma$, ΔT.

Percolation Studies in a microemulsion system

Electrical conductivity measurements of formulated microemulsion systems were carried out to learn more about the system's percolative behaviour, i.e., dynamic percolation (structural transitions from water in ionic liquid dispersion through bicontinuous microstructure towards the water in ionic liquid microemulsion). Variation of conductivity as a function of mass fraction was explored for percolation studies at different PLANTACARE® 810 – UP: [Bmim][PF$_6$] molar ratios (S=0.3 and 0.5), as shown in Figure 8.
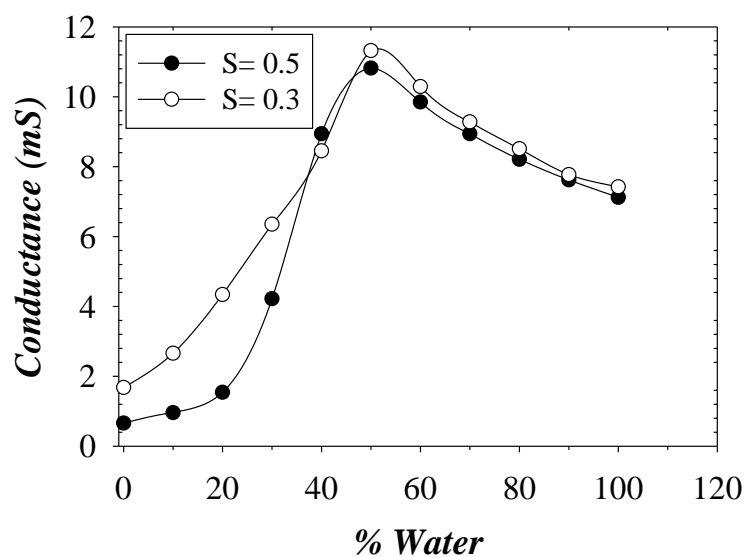
Figure 8. Variation of conductivity as a function of mass fraction of water at different PLANTACARE® 810 – UP: [Bmim][PF$_6$] molar ratio (S=0.3 and 0.5).

Similarly, the variation of conductivity as a function of the mass fraction was carried out for PLANTACARE® 818 – UP: [Bmim][PF$_6$] molar ratio (S=0.3 and 0.5). Resultant data has been illustrated below in Figure 9.
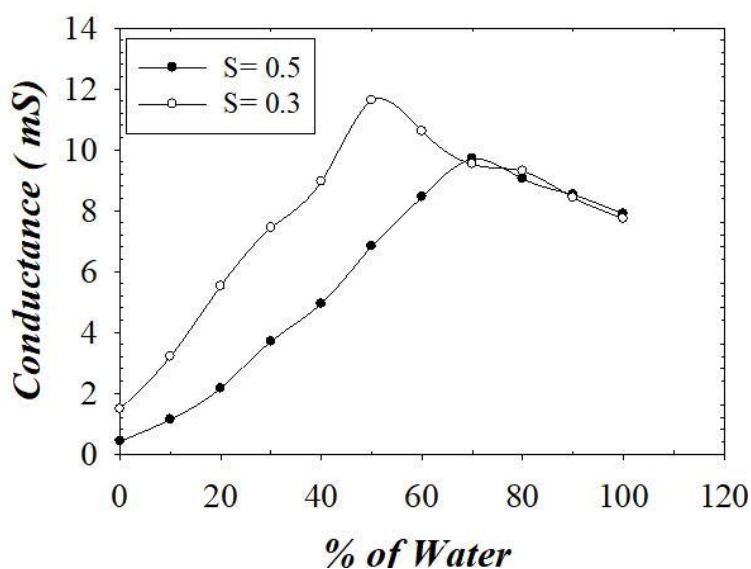

Figure 9: Variation of conductivity as a function of mass fraction of water at different PLANTACARE® 818 – UP: [Bmim][PF$_6$] molar ratio (S=0.3 and 0.5).

The values of electrical conductivity of water in IL dispersion grow constantly with an increase in water mass fraction, which is relevant with a rising number of ions in the system, as seen in the above graphs. Droplet collisions, charge transfer through a transitory merging of

droplets, and/or the creation of water channels are all factors that contribute to the rise in electrical conductivity. Water drifts to the outer phase as the system is diluted further with water, the curvatures adjust, and the conductivity rises.

The overall changes in conductance are not as rapid as in conventional microemulsion systems due to the significantly higher conductivity of ILs in contrast to the typical "oil" phase (and denoted as percolation in conductivity). During conductivity measurements, an increase of viscosity of the systems was observed, which may indicate a transition from microemulsion to liquid-crystalline phase. IL probably dissolves in water rather than forming IL/W microemulsion system, which is observed as almost a linear decrease of conductivity.

Percolation studies at different temperatures for PLANTACARE® 810 – UP: [Bmim][PF$_6$]

The Percolation studies by varying the conductivity as a function of the mass fraction at 25°C are shown in Figure 10.
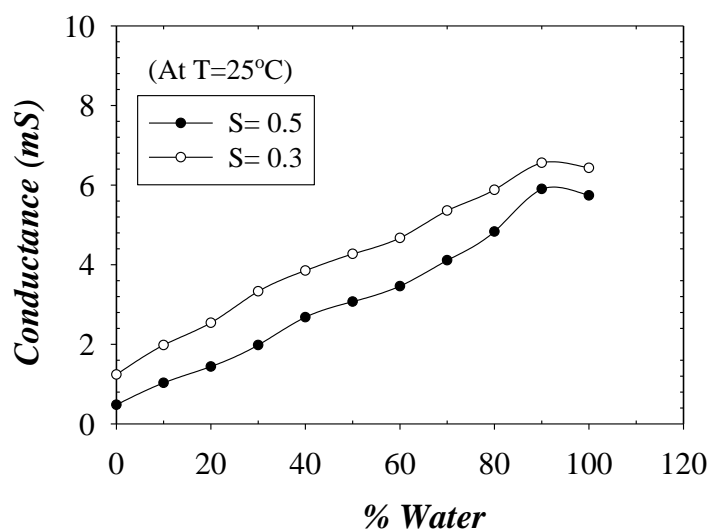

Figure 10. Variation of conductivity as a function of mass fraction of water at different PLANTACARE® 810 – UP: [Bmim][PF$_6$] molar ratio (S=0.3 and 0.5) at 25°C.

Similar observation is depicted that as the water mass fraction increases, the electrical conductivity of water in an ionic liquid dispersion also increases continuously. The kinetic energy, however, is insufficient due to the low temperature, resulting in slow movement of the ions. Percolation is seen when 90 % of the water is introduced at S=0.3 and S=0.5 when the system is held at 25°C, as shown in Figure 10. It means that the conductance rises slowly at low temperatures, and the process of droplet collisions is also slow. As a result, the CMC is

generated after 90 % of the water has been added. After the CMC is reached, adding additional water does not cause any more ions to move, therefore the conductivity remains constant since there are no more ions to collide or form micelles.

For percolation studies, variation of conductivity as a function of the mass fraction at different PLANTACARE® 810 – UP: [Bmim][PF$_6$] molar ratio (S=0.3 and 0.5) was investigated at 30°C. Resultant data has been illustrated below in Figure 11.
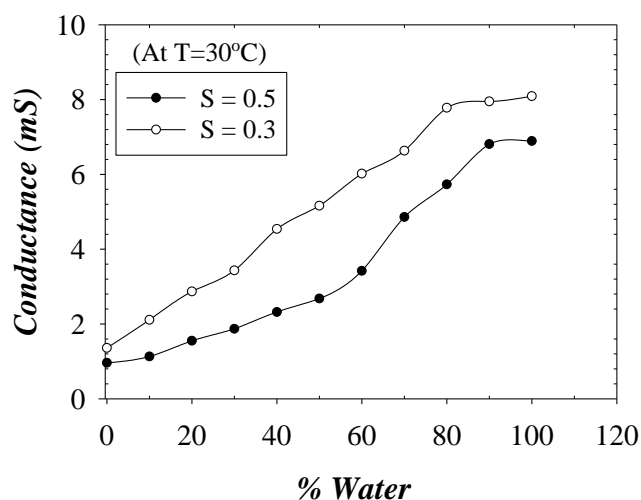

Figure 11. Variation of conductivity as a function of mass fraction of water at different PLANTACARE® 810 – UP: [Bmim][PF$_6$] molar ratio (S =0.3 and 0.5) at 30°C.

Similar results were obtained at 30°C, where we can see that as the concentration of water increases, the conductivity increases. In addition, it was discovered that when the molar ratio is S=0.3, conductivity increases significantly more than when it is S=0.5. Furthermore, we can see that as the conductivity varies, the viscosity increases.

For percolation studies, variation of conductivity as a function of the mass fraction at different PLANTACARE® 810 – UP: [Bmim][PF$_6$] molar ratio (S= 0.3 and 0.5) was investigated at 40°C. Resultant data has been illustrated below in Figure 12.
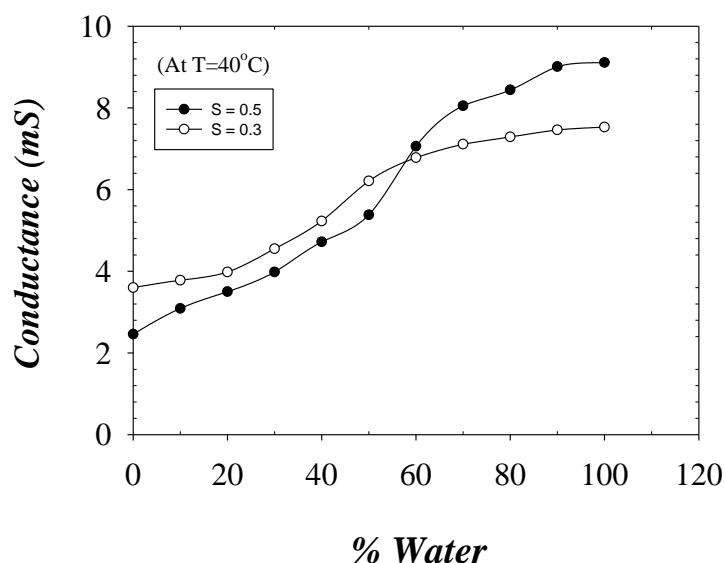
Figure 12. Variation of conductivity as a function of mass fraction of water at different PLANTACARE® 810 – UP: [Bmim][PF$_6$] molar ratio (S=0.3 and 0.5) at 40°C.

From Figure 12, it can be deduced that when the system is kept at 40°C, the conductivity rises quickly as the kinetic energy increases, causing the droplet interactions to become faster as well. Percolation is seen for S=0.3 when 50% of the water is added, and for S=0.5 when 60% of the water is added. It indicates that as the temperature rises, the micelles form more quickly. As a result, the percolating behaviour emerges quickly. For percolation studies, variation of conductivity as a function of the mass fraction at different PLANTACARE® 810 – UP: [Bmim][PF$_6$] molar ratio (S=0.3 and 0.5) was investigated at 50°C. Resultant data has been illustrated below in Figure 13.
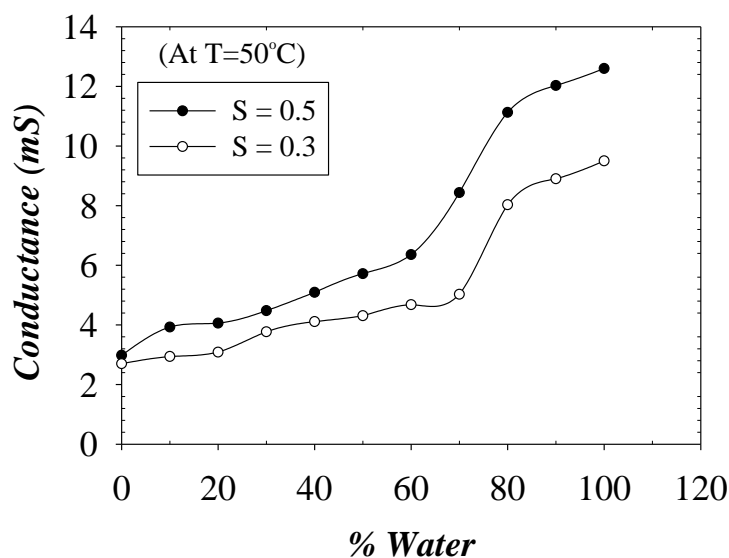
Figure 13: Variation of conductivity as a function of mass fraction of water at different PLANTACARE$^®$ 810 – UP: [Bmim][PF$_6$] molar ratio (S=0.3 and 0.5) at 50°C.

The percolation for S= 0.5 and S= 0.3 is evident when 80% of the water is injected, as shown in Figure 13. When the system is held at 50°C, the conductivity rises quickly as the kinetic energy increases, causing the droplets interactions to become fast.

Percolation studies by varying Ionic Liquid mass fraction (α) in PLANTACARE$^®$ 810 – UP: [Bmim][PF$_6$] system

Here, the percolation was studied by variation of conductivity as a function of mass fraction of PLANTACARE$^®$ 810 – UP: [Bmim][PF$_6$] system at 30°C by varying α. Resultant data has been illustrated below in Figure 14.
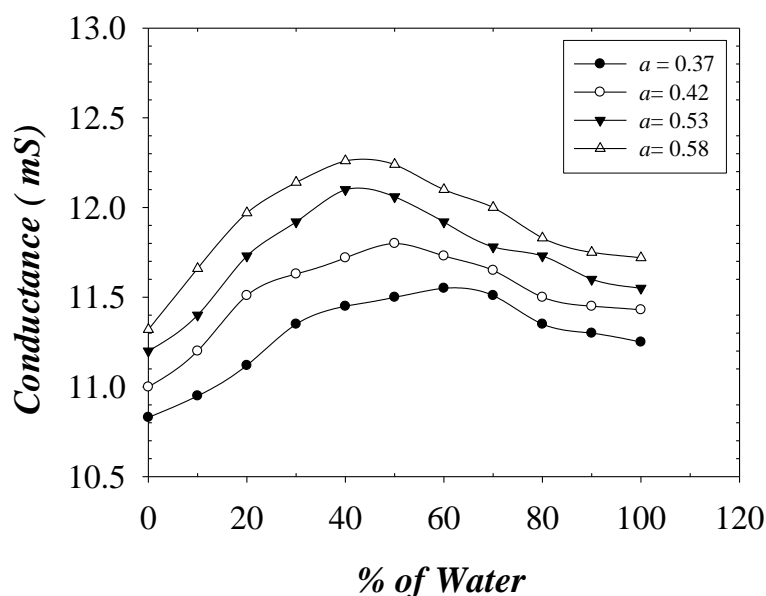

Figure 14. Variation of conductivity as a function of mass fraction of PLANTACARE$^®$ 810 – UP: [Bmim][PF$_6$] was investigated by varying α at 30°C.

The electrical conductivity of water in ionic liquid dispersion rises steadily as the water mass fraction rises, which is crucial as the number of ions in the system rises. As previously stated, the increase in conductivity is due to droplet collisions, charge transfer via temporary merging of droplets, and/or the creation of water channels. Water drifts to the outer phase as the system is diluted further with water, the curvatures adjust, and the conductivity rises. In addition to the foregoing results, we can see in Figure 14 that as the mass fraction of ionic liquid (α) rises, so does the conductance value. Also, by altering the mass percentage of the ionic liquids, the

viscosity of the systems increases, possibly indicating a shift from microemulsion to liquid-crystalline phase.

As seen in Figure 14, as the mass fraction of ionic liquids increases, more ions are present in the system, resulting in increased interactions, resulting in higher conductance. At $\alpha = 0.58$, when no water is added, the conductance is high, however at $\alpha = 0.37$, when water is added, the conductance is low. Similarly, as the ionic liquid mass fraction and the water volume fraction both increases, the conductance increases.

Despite the fact that the ionic liquids in the system have different mass fractions, percolation is expected at the same volume percent of water. For percolation investigations, two models have been proposed: the first, static percolation, is credited with the transformation into a bicontinuous structure with water channels, while the second, dynamic percolation, is credited with the development of clusters through water globule interactions. The dynamic percolation method was investigated in this work, and a distinct percolation phenomenon was detected in all plots, as illustrated in Figures 8-14.

It is interpreted from the plots that there is a sharp jump in conductance to an extent of ~6 orders of magnitude on just changing the concentration of water above a threshold water volume fraction. Initially, the value of conductance remains very low and suddenly it attains a high value. The conductance rises fiercely with an increase in the water volume fraction, due to the efficient transfer of ions through the water phase above the water percolation threshold. In addition to this, the interaction between droplets also plays a major role in producing the percolation effect. Furthermore, the percolation effect is largely influenced by the interaction between droplets. As water concentration rises, so does the population of water globules, and therefore there is an increase in the number of water globules.

As the concentration of water rises, the population of water globules rises as well, resulting in an increase in conductance. These findings are consistent with those reported in the literature (Ray et al., 1996; Hait et al., 2001; Schrodle et al., 2005; Naouli et al., 2011; Jeirani et al., 2012; Borkovec et al., 1988). The conductance values in a w/o microemulsion system are found to be low for low water fractions. This is attributed to a dynamic hopping mechanism (Ponton et al., 1991) of ions through the globules, with a sticky collision leading to droplet fusing above the percolation threshold. The kinetic energy of the water droplets in the oil continuum grows as the amount of water increases.

As a result, with low w/o ratios, each droplet spends less time in the vicinity of another droplet when colliding. If this duration is substantially shorter than the time required for hopping, the chances of conducting ions hopping from globule to globule are reduced, resulting in low conductance. Thus, at the threshold micelle concentration, a decrease in conductance with an increase in the water percentage supports the hoping mechanism rather than the sticky collision. As a result, depending on the droplet-droplet interaction, the percolation threshold value might be altered. As the droplet-droplet contact grows, its value falls.

Phase behaviour investigations of microemulsion systems containing ionic liquid/s, water, and industrial-grade sugar-based lauryl glucoside (and) cocamidopropyl betaine zwitterionic surfactant, on the other hand, were lacking from the literature. As a result, we developed a ternary microemulsion system with industrial-grade sugar-based lauryl glucoside (and) cocamidopropyl betaine zwitterionic surfactant/[Bmim][PF$_6$]/Water and investigated its phase behaviour in the current study. Figure 15 depicts the resulting information.
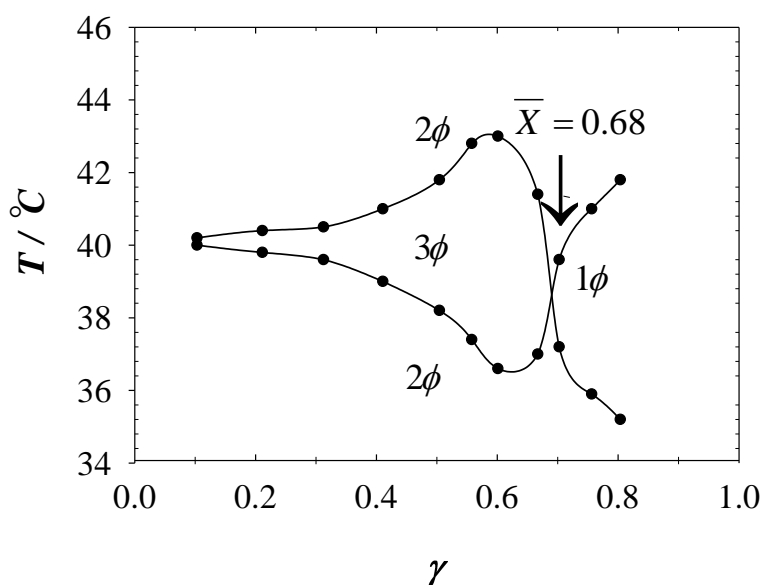

Figure 15. Fish-shaped phase diagram obtained for equal masses of water and IL [Bmim][PF$_6$], in presence of industrial-grade sugar-based lauryl glucoside (and) Cocamidopropyl betaine zwitterionic surfactant, i.e., PLANTACARE$^®$ K-55/ [Bmim][PF$_6$]/H$_2$O. The chosen IL mass fraction α corresponds to equal volumes of water and IL. T/°C represents the temperature and γ is the mass fractions of surfactant. 1Ø corresponds to one phase, 2Ø corresponds lower two phases (W/IL droplet μE), 2Ø corresponds upper two phases (IL/W droplet μE), and 3Ø corresponds to three-phase regions, respectively (Solanki & Patil, 2020).

Table 3 lists the typical parameters of the system's fish-shaped phase diagrams. The coordinates of the so-called fish head (lowest surfactant concentration at which a third middle phase appears) are γ_0 and T_0, while the coordinates of the fishtail are $\overline{\gamma}, \overline{T}$, IL volume fraction is represented by $\emptyset$, the maximum extension of surfactant concentration and temperature of the 3-phase body is denoted by $\Delta\gamma, \Delta T$ (Solanki & Patil, 2020).

Table 3. Characteristic parameters of the constructed Phase diagram

Microemulsion System	$\emptyset$	γ_0	$T_0/°C$	$\overline{\gamma}$	$\overline{T}/°C$	$\Delta\gamma$	$\Delta T/°C$
PLANTACARE®K- 55/ [Bmim][PF$_6$]/ H$_2$O	0.5	0.09	40.0	0.68	38.3	0.59	10.6

We have successfully created a microemulsion system combining industrial-grade sugar-based lauryl glucoside (and) cocamidopropyl betaine zwitterionic surfactant, i.e., PLANTACARE® K- 55 (UP-810) as a "greener option," as shown in Figure 15. However, the $\overline{X}$, which is the lowest surfactant concentration necessary to solubilize two immiscible solvents, is 0.68 for the developed microemulsion system PLANTACARE®K-55/ [Bmim][PF$_6$]/H$_2$O, as shown in the figure. Although a microemulsion can be made, the surfactant's efficiency in dissolving both water and oil ($\overline{X}$ value) is relatively high.

To formulate a microemulsion system, 68% sugar surfactant is required to solubilize two immiscible solvents, oil and water. The oil and water phases are at intermediate temperatures at T= $\overline{T}$ temperature and a very low surfactant concentration ($\gamma < \gamma_0$). As a result, the surfactant will have a high solubility in both water and oil, resulting in a surfactant-rich middle phase in equilibrium with an excess of oil and water. As the temperature rises, the middle phase expands until the full amount of water and oil is dissolved in this phase, giving birth to the $\overline{X}$ point, which is found to be 0.68.

The bottom phase (2$\emptyset$) is a water-rich phase at low temperatures, whereas the upper phase (2$\emptyset$) is oil (IL)-the surplus phase, where the surfactant forms oil-swollen micelles, also known as microemulsion droplets. When a surfactant is added to this binary combination, it becomes soluble in both phases. Later, as more surfactant is added, the concentration of the surfactant rises to the surfactant mass fraction, i.e., $\gamma = \gamma_0$, at this point, both the oil and water phases are saturated at the fish head. The third phase, known as the middle phase (3$\emptyset$) develops when the surfactant is added further (Solanki & Patil, 2020).

When the temperature is increased, the surfactant tends to get solubilized until the three-phase region (3∅) ($\gamma < \bar{\gamma}$) is observed. Further addition of the surfactant, now decreases the interfacial tension between the phases which results in the formation of a one-phase region (1∅) ($\gamma > \bar{\gamma}$) as shown in Figure 15. At higher temperatures, ionic liquid (oil) is a superior solvent for the surfactant, and IL-swollen reverse micelles form in an oil continuous phase, in equilibrium with a lower phase of excess IL.

2.4   Conclusions

As a function of temperature and surfactant mass fraction, the ternary phase behaviour of microemulsions containing water, hydrophobic ionic liquid (1-butyl-3-methylimidazolium hexafluorophosphate), and non-ionic sugar-based surfactants was investigated. We have concluded that the surfactant efficiency increases in terms of consumption, on formulating microemulsion system using sugar-based non-ionic surfactant as compared to that of conventional non-ionic surfactant. Also, we have employed zwitterionic surfactant with room temperature ionic liquid (RTIL) and water to formulate a microemulsion system.

Polarizing microscopy was used to examine the samples' microstructure. At lower temperatures, lamellar liquid crystalline phases (L_α) phases of *n*-Decyl *β*-D-maltoside/[Bmim][PF_6]/H_2O and *n*-Dodecyl *β*-D-maltoside/[Bmim][PF_6]/H_2O were observed in microemulsion systems. When a sugar-based non-ionic surfactant, PLANTACARE®810–UP, was utilised to produce a microemulsion system, polarisation microscopy studies demonstrated the absence of liquid crystalline phases (and high viscosity). Furthermore, the creation of percolation clusters of water droplets interacting in the oil medium causes percolation in a micellar phase of an oil-continuous microemulsion. At a constant temperature, the electrical conductivity of typical w/o systems remains low up to a specific proportion of water, then increases by two to three orders of magnitude after the water hits the system's threshold concentration (w_t) yielding a sigmoidal electrical conductivity–water content (% Water) curve. Our research shows that ionic liquids can be employed not only as a polar phase but also as an organic solvent replacement. Secondly, in formulating a microemulsion system, the sugar-based non-ionic surfactants we use play an important role as a greener alternative.